

Dynamical Age vs Spectral Age of the Lobes of Selected Giant Radio Sources (GRSs)

J. Machalski,¹ M. Jamrozy,¹ and D. J. Saikia²

¹*Astronomical Observatory, Jagiellonian University, Krakow, Poland*

²*National Centre for Radio Astrophysics, TIFR, Pune, India*

Abstract. Dynamical ages of the opposite lobes determined *independently* of each other suggest that their ratios are between ~ 1.1 to ~ 1.4 . Demanding similar values of the jet power and the radio core density for the same GRS, we look for a *self-consistent* solution for the opposite lobes, which results in different density profiles along them found by the fit. A comparison of the dynamical and spectral ages shows that their ratio is between ~ 1 and ~ 5 , i.e. is similar to that found for smaller radio galaxies. Two causes of this effect are pointed out.

1. Introduction

The dynamical ages of the opposite lobes of 10 selected giant radio sources are estimated using the DYNAGE algorithm of Machalski et al. (2007) and compared with their spectral ages determined and studied by Jamrozy et al. (2008). The DYNAGE algorithm is an extension of the analytical model for the evolution of FR II type radio sources combining the dynamical model of Kaiser & Alexander (1997) with the model for expected radio emission from a source under the influence of energy loss processes published by Kaiser, Dennett-Thrope, & Alexander 1997; hereafter referred to as KDA). This algorithm allows to determine the values of four of the model parameters, i.e. the jet power, Q_{jet} , central core density, ρ_0 , energy distribution of the relativistic particles injected into the lobe via acceleration processes and described by the spectral index α_{inj} , and the lobe's age, t . The determination of their values is made possible by the fit to the observational parameters of a lobe: its length, D , axial ratio (geometry), R_T , normalization and slope of its radio spectrum, i.e. the radio luminosity, $P_{\nu,i}$, at a number of observing frequencies $\nu=1,2,3\dots$. The values of other free parameters of the model have to be assumed.

2. Dynamical Model and the Age Solutions

Three basic relations of the model are:

$$\rho(r) = \rho_0(r/a_0)^{-\beta} \quad \text{for } r \geq a_0, \quad (1)$$

$$L_{\text{jet}}(t) = \text{const} \left(Q_{\text{jet}}/\rho_0 a_0^\beta \right)^{1/(5-\beta)} t^{3/(5-\beta)} \quad \text{and,} \quad (2)$$

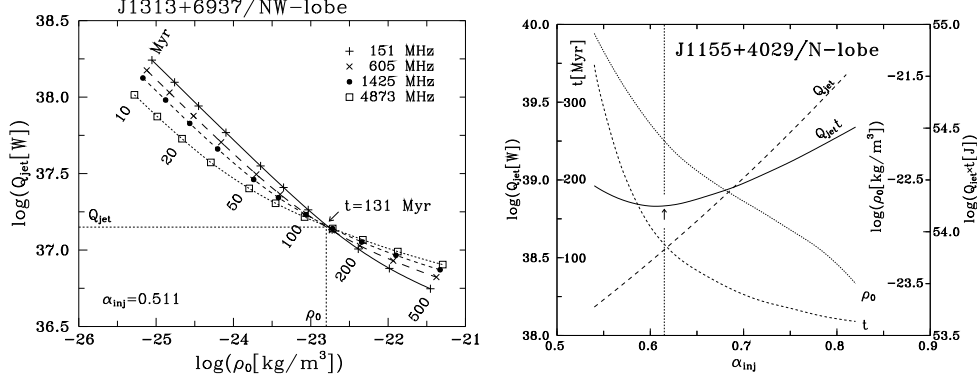


Figure 1. Left: A set of $Q_{\text{jet}}(t)$ and $\rho_0(t)$ solutions at the four observing frequencies for a lobe of J1313+6937. Right: The dependence of Q_{jet} , $Q_{\text{jet}} \times t$, and ρ_0 on α_{inj} for a lobe of J1155+4029.

$$P_\nu = \frac{1}{6\pi} \int_{(t_{\text{min}})}^t \sigma_{\text{TC}} u_{\text{B}} Q_{\text{jet}} \frac{\gamma^3}{\nu} n(\gamma, t_i) V(t_i) dt_i \quad (3)$$

2.1. Independent Age Solution (3 steps)

1) Assuming the values of remaining free parameters of the model (cf. Machalski et al. 2009) – for given values of $p(\alpha_{\text{inj}})$ and t equating

$$L_{\text{jet}} \stackrel{[\text{Equation 2}]}{\cong} D_{\text{obs}} / \sin \Theta$$

and

$$P_\nu \stackrel{[\text{Equation 3}]}{\cong} P_{\nu, \text{obs}},$$

the DYNAGE fits the values of $Q_{\text{jet}}(\alpha_{\text{inj}}, t, P_\nu)$ and $\rho_0(\alpha_{\text{inj}}, t, P_\nu)$.

2) Performing step 1) for all P_ν chosen to represent the lobe's spectrum, we have $t(\alpha_{\text{inj}})$, $Q_{\text{jet}}(\alpha_{\text{inj}})$, and $\rho_0(\alpha_{\text{inj}})$ (Figure 1, left).

3) The steps 1) and 2) are repeated for a number of α_{inj} values searching for its value which provides a minimum of the kinetic energy delivered to the lobe at the age t , i.e. $Q_{\text{jet}} \times t$ (Figure 1, right). This, in turn, provides the final solutions of t , Q_{jet} , and ρ_0 , as well as of their derivative parameters (see Table 4 in Machalski et al. 2007)

Objections: Independent age solutions give *different* ages of the opposite lobes which is shown in Figure 2 (left). The differences are larger than expected kinematic age differences due to a projection of the jet's axis.

From Equation (2) we have

$$t = \left(\frac{D}{c_1} \right)^{(5-\beta)/3} \left(\frac{\rho_0 a_0^\beta}{Q_{\text{jet}}} \right)^{1/3}. \quad (4)$$

For the same source (consisting of two lobes) we note that

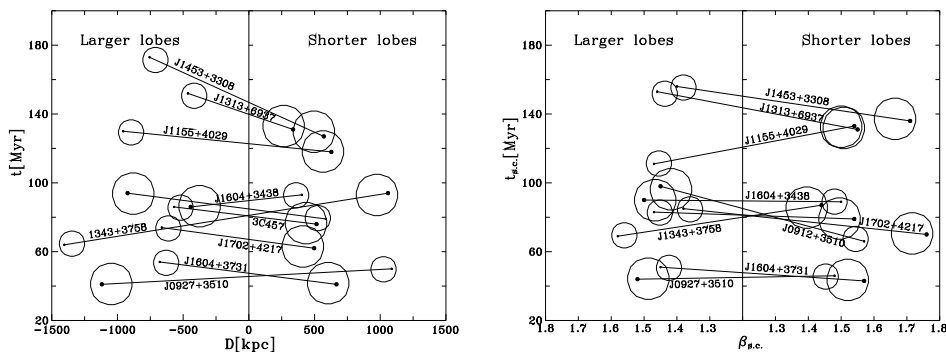


Figure 2. Left: Schematic display of the ‘independent solution’ of age, t vs length of the lobes. Right: Similar display of the ‘self-consistent’ solution (the same Q_{jet} and ρ_0 forced for both lobes) of age, $t_{\text{s.c.}}$, vs exponent of the external density profile. In both diagrams longer lobes are on the left side, while shorter ones – on the right side of the diagram. Larger circles indicate a brighter lobe; smaller circles – a fainter one.

- larger D suggests older t , and calculations show that (usually)
- larger D accompanies a higher value of ρ_0 than that for shorter D .

Thus, substitution of $\langle \rho_0 \rangle$ into Equation (4) and a change of β can lower t . However, this does not satisfy Equation (3) where the lobe’s radiation is controlled by Q_{jet} and α_{inj} . Therefore we look for self-consistent age solution.

2.2. Self-Consistent Age Solution

Let $\rho(r = D) \equiv \rho_a$; thus from Equation (1)

$$\rho_0 \left(\frac{D}{a_0} \right)^{-\beta} = \langle \rho_0 \rangle \left(\frac{D}{a_0} \right)^{-\beta_{\text{s.c.}}} \quad \text{we have } \beta_{\text{s.c.}}$$

Substitution of $\beta_{\text{s.c.}}$ into Equation (4) gives the ‘self-consistent’ age

$$t_{\text{s.c.}} = \left(\frac{D}{c_1} \right)^{(5-\beta_{\text{s.c.}})/3} \left(\frac{\langle \rho_0 \rangle a_0^{\beta_{\text{s.c.}}}}{\langle Q_{\text{jet}} \rangle} \right)^{1/3} \quad (5)$$

The ‘self-consistent’ ages of the opposite lobes calculated from Equation (5) are plotted vs $\beta_{\text{s.c.}}$ in Figure 2 (right).

3. Discussion of the Results

1. In 7 of 10 GRSs the brighter lobe is found to be younger than the opposite, fainter one, but
2. dynamical ages of opposite lobes differ between themselves more than it is expected due to the kinematic age difference related to a projection of the jet’s axis toward the observer.

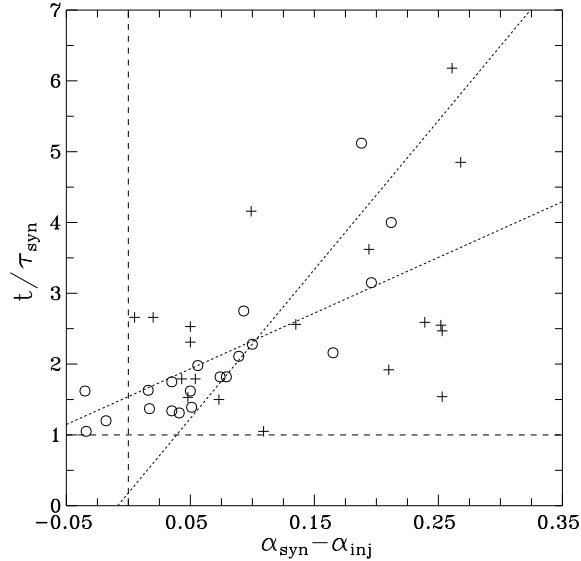


Figure 3. Ratio of the dynamical age of the lobe, t , and their synchrotron age, τ_{syn} , vs the difference $\alpha_{\text{syn}} - \alpha_{\text{inj}}$. Circles indicate the ratio of t , and τ_{CI} , while crosses indicate the ratio of t , and τ_{JP} . The value of τ_{CI} and τ_{JP} are given in Jamrozy et al. (2008). The two dotted lines show linear regression lines on each of the two coordinates.

3. The apparent asymmetries in the lobes' length, their luminosity, and age are likely to be due to different propagation conditions of the jets through an external medium.
4. Assuming different exponents β in Equation (1) in opposite jet's directions, the age difference usually decreases, however still remaining larger than that due to the kinematic effect.
5. Expected exponents $\beta_{\text{s.c.}}$ for the shorter lobes are higher than those for the larger ones.
6. Differences of age $t_{\text{s.c.}}$ can be levelled by a departure from the equipartition between the energy densities of magnetic fields and relativistic particles. An increase of $r \equiv u_{\text{B}}/u_{\text{c}}$ results in increase of the lobe's age; however it is connected with a corresponding decrease of the jet power. A decrease of r acts inversely.
7. A ratio of the dynamical age to the spectral age is between 1 and 5. This is caused by (i) a difference between the injection spectral indices determined using the DYNAGE algorithm in the dynamical analysis and the SYNAGE algorithm of Murgia (1996) in the spectral-ageing analysis (shown in Figure 3), and (ii) a different influence of the axial ratio of the lobes in the estimation of the dynamical age and the spectral age.

In Machalski, Jamrozy, & Saikia (2009) arguments are given that DYNAGE can better take account of radiative effects at low frequencies than SYNAGE, and

the age solutions should be better than those found with the classical spectral-ageing analysis because the expansion parameters are connected to actual geometry of the lobes for each specific GRS. The DYNAGE algorithm is especially effective for sources at high redshifts for which an intrinsic spectral curvature is shifted to low frequencies.

References

- Jamrozy, M., Konar, C., Machalski, J., & Saikia, D. J. 2008, MNRAS, 385, 1286
Kaiser, C. R., & Alexander, P. 1997, MNRAS, 286, 215
Kaiser, C. R., Dennett-Thorpe, J., & Alexander, P. 1997, MNRAS, 292, 723 (KDA)
Machalski, J., Chyży, K.T., Stawarz, L., & Koziel, D. 2007, A&A, 462, 43
Machalski, J., Jamrozy, M., & Saikia, D. J., 2009, MNRAS, 395, 812
Murgia, M. 1996, Ph.D Laurea Thesis, University of Bologna